Full title:

Transcriptomic meta-analysis of non-Hodgkin's B-cell lymphomas reveals reliance on pathways associated with the extracellular matrix

Short title:

Transcriptomic meta-analysis of non-Hodgkin's B-cell lymphomas

Authors: Naomi Rapier-Sharman[1], Jeffrey Clancy[1], and Brett E. Pickett[1,*]

[1] Department of Microbiology and Molecular Biology, Brigham Young University, Provo, UT 84602

*Corresponding author; email: brett_pickett@byu.edu, phone: 801-422-2506, address: 3141 LSB Provo, UT 84602-1050

Abstract

Approximately 450,000 cases of Non-Hodgkin's lymphoma are diagnosed annually worldwide, resulting in ~240,000 deaths. An augmented understanding of the common mechanisms of pathology among relatively large numbers of B-cell Non-Hodgkin's Lymphoma (BCNHL) patients is sorely needed. We consequently performed a large transcriptomic meta-analysis of available BCNHL RNA-sequencing data from GEO, consisting of 322 relevant samples across ten distinct public studies, to find common underlying mechanisms across BCNHL subtypes. The study was limited to GEO's publicly available human B-cell RNA-sequencing datasets that met our criteria, and limitations may include lack of diversity in ethnicities and age groups. We found ~10,400 significant differentially expressed genes (FDR-adjusted p-value < 0.05) and 33 significantly modulated pathways (Bonferroni-adjusted p-value < 0.05) when comparing lymphoma samples to non-diseased samples. Our findings include a significant class of proteoglycans not previously associated with lymphomas as well as significant modulation of extracellular matrix-associated proteins. Our drug prediction results yielded new candidates including ocriplasmin and collagenase. We also used a machine learning approach to identify the BCNHL biomarkers YES1, FERMT2, and FAM98B, novel biomarkers of high predictive fidelity. This meta-analysis validates existing knowledge while providing novel insights into the inner workings and mechanisms of B-cell lymphomas that could give rise to improved diagnostics and/or therapeutics. No external funding was used for this study.

Introduction

Lymphomas are cancers of the blood. In 2016, there were 461,000 cases of Non-Hodgkin's lymphoma worldwide, resulting in 240,000 deaths (1). Among non-Hodgkin's lymphomas, only ~10-15% are T-cell lymphomas, while the remaining 85-90% are B-cell malignancies (2). B-cell Non-Hodgkin's Lymphomas (BCNHLs) pose a significant disease burden worldwide. BCNHL subtypes include Burkitt's lymphoma, nodal, extra-nodal, and splenic marginal-zone B-cell

lymphomas, follicular lymphoma, diffuse large B-cell lymphoma, mantle cell lymphoma, post-transplantation lymphoproliferative disorders, small lymphocytic lymphoma, lymphoblastic lymphoma, lymphoplasmacytic lymphoma, and lymphomatoid granulomatosis (2). B-cell lymphomas are dependent on their extracellular environment for activation and transformation into malignancies, including antigen activation of the B-cell receptor, canonical B-cell growth signals which are also essential to the maturation of healthy B-cells, and signals delivered by other immune cells in the follicular/germinal center lymphoma microenvironment (3).

The research community has dedicated extensive effort to identify the attributes that characterize cancers across all subtypes. Specifically, it has been suggested previously that all cancers share the following traits: selective proliferative advantage, altered stress response, vascularization, invasion and metastasis, metabolic rewiring, immune modulation, and an abetting microenvironment (4,5). One example of a molecular mechanism that is common in cancer is malignant development through TP53 mutation, with multiple mutations in the TP53 being associated with hundreds of cancer subtypes (6). Though not every gene-mechanism pairing will be found across malignant cells like TP53, it is logical to assume that identifying shared genes and mechanisms by meta-analyzing previous research in a focused set of related cancer subtypes can be beneficial. We can therefore leverage known mechanisms from well-studied subtypes to enable quicker, less expensive mechanism discovery for understudied subtypes. This approach could potentially enable researchers to develop safe and effective treatments.

The widespread adoption of RNA-sequencing (RNA-seq) has opened new frontiers in disease research. Rather than identifying and characterizing individual proteins, transcriptomic meta-analyses can provide a mechanistic snapshot of the many upregulated or downregulated genes that are affected in response to a given stimulus, such as lymphoma. Monitoring these transcriptional patterns can aid in the identification of genes that could be worth further experimental investigation due to their selective modulation in diseased samples. Though the

RNA-sequencing samples in the current study were previously published, compiling them into a meta-analysis can grant us new insights into disease mechanisms by increasing the signal of significant genes and reducing the statistical "noise" caused by outliers.

The aim of this study was to identify some of the shared underlying molecular mechanisms and biomarkers of B-cell lymphomas by performing a meta-analysis of transcriptomic data from publicly available B-cell Non-Hodgkin's Lymphomas (BCNHLs) clinical samples. We expect our analysis to validate past findings of B-cell cancer mechanisms and uncover mechanisms that have not been previously associated with BCNHL.

Results

We acquired our BCNHL samples from the NCBI Gene Expression Omnibus (GEO) using the search term, "b-cell lymphoma" with the goal of finding B-cell non-Hodgkin's lymphoma samples and healthy B-cell controls. We excluded non-human samples, cell lines, formalin-fixed paraffin-embedded tissues, gene expression microarray experiments, single-cell (10X) RNA-sequencing experiments, xenografts, samples known to be infected with EBV and KSHV, and samples which contained more diverse cell types (i.e., whole blood, lymph node, PBMCs, brain, etc.). We intentionally decided to not include multiple myeloma, leukemia, and Hodgkin's lymphoma samples in favor of focusing on B-cell non-Hodgkin's lymphomas. We then located more healthy B-cell control samples from BCNHL-unrelated studies to even out case and control numbers, the final three studies cited in Table 1. Our final dataset included a total of 322 samples (134 BCNHL samples and 188 healthy B-cell controls) from ten studies (Fig 1, Table 1, S1 File) (7–18). The samples included in our meta-analysis were all clinical samples. The risk of synthesizing study results and accounting for heterogeneity were reduced due to the lack of treatment metadata and patient outcome data as input to our analysis. Given that the aim of this study was to compare the maximum number of BCNHL samples to healthy B-cells, the only source of heterogeneity that we

are concerned with is the distribution of BCNHL samples across the included subtypes. Our study was limited to GEO's publicly available human B-cell RNA-sequencing datasets that met our criteria, and limitations may include lack of diversity in ethnicities and age groups.

Figure 1. PRISMA flow diagram for transparent reporting of meta-analysis study selection. Contains a study-by-study breakdown of selection criteria. All studies included were retrieved from the Gene Expression Omnibus (GEO) database hosted by NCBI.

Table 1. Study-based origin of samples included in the meta-analysis.

Sample Phenotype	Single End or Paired End Reads	GEO Accession #	Relevant Samples
Large B-Cell Lymphoma	Paired End	GSE153437 (7)	25
Diffuse Large B-Cell Lymphoma	Paired End	GSE130751 (8)	63
B-Cell Lymphoma + Healthy	Single End	GSE110219 (9)	2
Diffuse Large B-Cell Lymphoma	Paired End	GSE95013 (10)	28
Follicular Lymphoma + Healthy	Paired End	GSE62241 (11,12)	14
Diffuse Large B-Cell Lymphoma	Paired End	GSE50514 (13)	7
Healthy	Paired End	GSE45982 (14,15)	8
Healthy	Single End	GSE92387 (16)	12
Healthy	Paired End	GSE118254 (17)	147
Healthy	Paired End	GSE110999 (18)	16

The samples used in this meta-analysis all originate from publicly-available RNA-sequencing projects and can be found on NCBI's GEO.

We began by trimming, mapping, and quantifying the reads prior to calculating the significant differential gene expression when comparing the Lymphoma to the non-diseased control samples. This comparison returned ~13,800 significant differentially expressed genes (DEGs) (Figs 2 and 3, Table 2, S2 File). We then ranked this list by the FDR-corrected p-value for each gene. We observed that the top 20 DEGs include accepted biomarkers of various Lymphomas. Specifically, we confirmed several genes that have previously been explored or characterized in various subtypes of BCNHL including Apolipoprotein C1 (APOC1; logFC = 6.93, FDR = 8.55×10^{-117}) and Vascular cell adhesion molecule 1 (VCAM1; logFC = 7.85, FDR = 2.29×10^{-120}) to be upregulated in BCNHLs. We also found two pathological BCNHL genes, C-C motif chemokine ligand 18 (CCL18; logFC = 10, FDR = 3.74×10^{-123}) and C-X-C motif chemokine ligand 9

(CXCL9; logFC = 11, FDR = 4.31×10^{-141}) to be upregulated in BCNHL as compared to healthy B-cells.

Figure 2. Visualization of Differentially Expressed Genes and Gene Ontologies.
Differentially expressed gene volcano plot. Green dots represent genes which were not significantly differentially expressed between healthy B-cells and BCNHL, while the salmon and blue dots represent underexpressed and overexpressed genes respectively.

Figure 3. Visualization of Gene Ontology Terms.
Gene ontology visualization. Each rectangle represents a gene ontology term found in the KEGG Brite gene ontology hierarchy. The size of each rectangle corresponds to the number of BCNHL differentially expressed genes present in that category. The color of each rectangle corresponds to the average $\log_2$ fold change of the genes included in that gene ontology. No KEGG Brite gene ontologies were found to be significantly differentially expressed by the bc3net hypergeometric enrichment.

Table 2. Top 20 significant differentially expressed genes.

	Gene Symbol	Ensembl ID	Log_2 Fold Change	FDR-corrected p-value
1	LUM	ENSG00000139329	11.1	1.11×10^{-145}
2	CXCL9	ENSG00000138755	11	4.31×10^{-141}
3	C1QC	ENSG00000159189	9.65	2.70×10^{-132}
4	C1QA	ENSG00000173372	9.54	2.03×10^{-123}
5	CCL18	ENSG00000278167	10	3.74×10^{-123}
6	VCAM1	ENSG00000162692	7.58	2.29×10^{-120}
7	C1QB	ENSG00000173369	9.4	8.19×10^{-119}
8	APOC1	ENSG00000130208	6.93	8.55×10^{-117}
9	AL512646.1	ENSG00000203396	-15.6	2.24×10^{-115}
10	CCL19	ENSG00000172724	8.48	1.27×10^{-111}
11	SLAMF8	ENSG00000158714	7.77	4.01×10^{-111}
12	COL3A1	ENSG00000168542	10.1	1.67×10^{-110}
13	TCIM	ENSG00000176907	8.07	7.86×10^{-110}
14	RARRES2	ENSG00000106538	7.25	8.21×10^{-109}
15	CXCL13	ENSG00000156234	8.8	1.72×10^{-107}
16	SPARCL1	ENSG00000152583	7.24	6.42×10^{-107}
17	PTGDS	ENSG00000107317	7.69	1.07×10^{-105}
18	COL1A2	ENSG00000164692	8.33	3.70×10^{-102}
19	CXXC5	ENSG00000171604	-2.73	3.70×10^{-102}
20	C1R	ENSG00000159403	4.7	1.41×10^{-100}

The top 20 differentially expressed genes between BCNHL and healthy B-cell samples. This list includes genes that have been previously researched in conjunction with BCNHL as well as novel genes.

We then examined the highest-ranking differentially expressed genes from our meta-analysis to identify gene-based mechanisms of disease. The first gene we observed using this approach was Lumican (LUM), which is a member of the small leucine-rich proteoglycans (SLRPs) (19), and was substantially upregulated in lymphoma (log_2 fold change = 11.1, FDR p-value = 1.11×10^{-145}). In addition, the larger family of SLRPs appears to play a role in BCNHL (Table 2). Specifically, our data show that 12/18 SLRPs are expressed in cancerous B-cells, and that 11/12 B-cell-expressed SLRPs are significantly differentially expressed in BCNHL samples. We found that overall, the SLRP fold changes substantially differed (9/12 expressed SLRPs are upregulated, 2/12 are downregulated, 1/12 had no significant change), with the genes encoding SLRPs (especially Classes I and V) being well represented in the B-cell lymphoma transcriptome.

Table 3. Differential expression of members of the Small Leucine-Rich Proteoglycan Family (SLRPs).

SLRP Class	Name	Log_2 Fold Change	FDR-corrected p-value
Class I	DCN	2.88	1.67×10^{-41}
	BGN	7.88	3.22×10^{-95}
	ASPN	3.09	2.27×10^{-25}
	ECM2	2.1	1.44×10^{-17}
	ECMX	NP	NP
Class II	FMOD	5.71	3.86×10^{-61}
	LUM	11.1	1.11×10^{-145}
	PRELP	0.617	1.54×10^{-4}
	KERA	NP	NP
	OMD	NP	NP
Class III	EPYC	NP	NP
	OPTC	NP	NP
	OGN	NS	NS
Class IV	CHAD	-3.49	1.33×10^{-24}
	NYX	NP	NP
	TSKU	1.37	1.62×10^{-16}
Class V	PODN	1.66	5.70×10^{-10}
	PODNL1	-1.49	3.15×10^{-11}

Out of the 18 members of the SLRP family, 12 are expressed in B-cells and 11 are significantly differentially expressed between BCNHL and healthy B-cells. This is a novel finding.
*NS = not significant; NP = not present.

Complement proteins are typically regarded as components of the innate immune system, which bind to antigen-antibody complexes to facilitate the formation of the membrane attack complex.

We found that genes encoding the Complement C1q A (C1QA; logFC = 9.54, FDR = 2.03×10^{-123}), Complement C1q B (C1QB; logFC = 9.4, FDR = 8.19×10^{-119}) and Complement C1q C (C1QC; logFC = 9.65, FDR = 2.7×10^{-132}) chains were all dramatically and significantly upregulated in BCNHL.

We detected AL512646.1 (also known as LOC100128906 and as a WDR45-like pseudogene) as differentially expressed by B-cell non-Hodgkin's lymphoma samples, a novel observation which was somewhat unexpected. Though AL512646.1 is annotated as a pseudogene, the RNA-sequencing data shows that it is downregulated in at least a subset of BCNHLs ($\log_2$FC = -15.1), and it has not been previously associated with cancer.

Next, we used the DRIMSeq algorithm to determine which genes had significant differences in the presence of splice variants between case and control samples. This analysis returned 320 genes for which splice variants were significantly different (Table 4, S3 File). Apolipoprotein E (APOE) was the most statistically significant splice variant (Lr [likelihood ratio] = 4470, # of alternate splice variants = 4, adjusted p-value = 0). Specifically, we observed the expression of APOE transcripts ENST00000252486, ENST00000425718, ENST00000434152, ENST00000446996, and ENST00000485628 to significantly differ between non-Hodgkin's lymphoma and non-diseased B-cells.

Table 4. Top 20 most significant splice variants (by gene).

Gene symbol	Ensembl ID	Lr*	# of Alternate Transcripts	Adjusted P-value
APOE	ENSG00000130203	4470	4	0
COL1A1	ENSG00000108821	1520	12	5.56×10^{-315}
COL27A1	ENSG00000196739	1060	7	6.71×10^{-220}
RPL5	ENSG00000122406	1040	10	3.86×10^{-214}
KLF6	ENSG00000067082	961	6	7.41×10^{-201}
SRSF6	ENSG00000124193	954	5	1.56×10^{-200}
CYBRD1	ENSG00000071967	931	6	2.17×10^{-194}
PLEKHM1P1	ENSG00000214176	924	5	3.78×10^{-194}
VCP	ENSG00000165280	912	6	2.37×10^{-190}

DDX6	ENSG00000110367	872	7	8.01×10^{-181}
THRAP3	ENSG00000054118	846	3	6.63×10^{-180}
FCGR2B	ENSG00000072694	771	4	1.75×10^{-162}
CHI3L1	ENSG00000133048	715	4	2.40×10^{-150}
IFITM3	ENSG00000142089	691	3	2.53×10^{-146}
ADAM28	ENSG00000042980	719	11	4.56×10^{-144}
CIB1	ENSG00000185043	662	2	2.04×10^{-141}
ZNF318	ENSG00000171467	645	3	1.88×10^{-136}
RPS28	ENSG00000233927	621	3	3.10×10^{-131}
CCDC124	ENSG00000007080	549	3	1.14×10^{-115}
ZNF335	ENSG00000198026	545	3	8.02×10^{-115}

Significantly differentially expressed splice variants sorted by gene.
*Lr = likelihood ratio

We also observed that Collagen type I alpha 1 chain (COL1A1) had significant splice variants (Lr = 1520, # of alternate splice variants = 12, adjusted p-value = $5.55999999807983 \times 10^{-315}$). Interestingly, our study also found that the COL1A1 gene was significantly upregulated in BCNHL (logFC = 3.73, FDR = 9.78×10^{-48}). We also observed novel significant splice variants in Collagen type XXVII alpha 1 chain (COL27A1), which was found to be significant in BCNHL (Lr = 1060, # of alternate splice variants = 7, adjusted p-value = 6.71×10^{-220}).

We then wanted to determine which functional terms in the Gene Ontology were over-represented by the list of DEGs in BCNHL. The Camera algorithm checked 14,901 terms (including gene ontologies and human phenotypes) for enrichment against the significant differentially expressed genes that we generated with edgeR. Although there were 482 results (p-value < 0.05), none remained significant after multiple hypothesis correction (S4 File). The lack of significant results is somewhat expected given the overall molecular heterogeneity of BCNHL subtypes. To visualize the gene ontology changes, we used a hypergeometric enrichment algorithm that applied a p-value cutoff of 0.05. We then averaged the edgeR fold-change values for the genes of each gene ontology in the KEGG Brite hierarchy and plotted the enrichment results using the R Treemap package to better understand the contribution of various terms to the overall list of DEGs (Fig 3).

To better understand the results of our analysis at a more mechanistic level, we used the signaling pathway impact analysis (SPIA) algorithm to identify intracellular signaling pathways that play important roles in Lymphoma. This pathway analysis generates a null distribution through bootstrapping to identify pathways that are significantly modulated when comparing sets of samples. Our analysis revealed 33 significantly modulated pathways between lymphoma B-cells and non-diseased B-cells (Table 5, S5 File). Specifically, we observed eight pathways that

were involved with the extracellular matrix and connective tissue in general, including Integrin signaling pathway, Extracellular matrix organization, ECM-receptor interaction, Focal adhesion, Integrins in angiogenesis, integrin signaling pathway, Collagen formation, and Collagen degradation. The upregulation of these pathways indicate that BCNHL likely benefits from modulations to the extracellular matrix.

Table 5. Significant differentially modulated signaling pathways.

	Name	pSize	NDE	tA	pGFWER	Source Database
1	Integrin signalling pathway	99	86	114.394	2.39×10^{-5}	Panther
2	Extracellular matrix organization	204	180	80.7398395	3.14×10^{-5}	Reactome
3	ECM-receptor interaction	70	64	77.659	4.47×10^{-5}	KEGG
4	Staphylococcus aureus infection	32	29	110.568396	0.000503428	KEGG
5	Complement and coagulation cascades	36	32	37.5461944	0.000674242	KEGG
6	Urokinase-type plasminogen activator (uPA) and uPAR-mediated signaling	28	25	130.821315	0.000740169	NCI
7	Cytokine-cytokine receptor interaction	168	140	98.294	0.000780995	KEGG
8	Focal adhesion	182	150	236.615459	0.001133449	KEGG
9	PI3K-Akt signaling pathway	271	221	260.046197	0.001344307	KEGG
10	Complement cascade	29	27	102.278583	0.001440498	Reactome
11	Systemic lupus erythematosus	17	15	67.4577222	0.001616635	KEGG
12	b cell survival pathway	22	19	26.576	0.00167109	BioCarta
13	Small cell lung cancer	78	64	121.170067	0.001930414	KEGG
14	Integrins in angiogenesis	52	41	146.143424	0.00285984	NCI
15	Olfactory transduction	93	74	-148.8965	0.002966626	KEGG
16	integrin signaling pathway	37	29	77.0156667	0.003336442	BioCarta
17	erk and pi-3 kinase are necessary for collagen binding in corneal epithelia	34	26	166.268917	0.003755165	BioCarta
18	RNA Polymerase I Promoter Clearance	85	72	-40.156	0.004307328	Reactome
19	Initial triggering of complement	15	14	44.508	0.004480759	Reactome
20	RNA Polymerase I Promoter Opening	39	34	-40.907	0.004675938	Reactome
21	RHO GTPases activate PKNs	67	57	39.779	0.004802382	Reactome
22	DNA Damage/Telomere Stress Induced Senescence	61	52	32.7708077	0.004980633	Reactome
23	Creation of C4 and C2 activators	7	7	27.365	0.005633091	Reactome
24	Collagen formation	66	63	26.4272897	0.006045837	Reactome
25	Activated PKN1 stimulates transcription of AR (androgen receptor) regulated genes KLK2 and KLK3	41	35	39.094	0.006675281	Reactome
26	MET activates PTK2 signaling	18	16	63.573	0.007079287	Reactome
27	Collagen degradation	17	15	131.8905	0.008037505	Reactome
28	MET promotes cell motility	28	24	97.5445	0.00808298	Reactome
29	Regulation of IGF Activity by IGFBP	11	10	25.958725	0.008404989	Reactome
30	Classical antibody-mediated complement activation	5	5	27.354	0.008619298	Reactome
31	Serotonin Neurotransmitter Release Cycle	11	9	-13.301889	0.015608196	Reactome
32	Class A/1 (Rhodopsin-like receptors)	81	77	5.908	0.026176599	Reactome
33	Peptide ligand-binding receptors	79	75	5.84	0.040928099	Reactome

The significantly differentially modulated pathway results. Included are nine extracellular matrix-associated pathways.

*Abbreviations: psize = number of genes in pathway. NDE = number of genes from pathway which were differentially expressed. tA = measure of change between healthy and lymphoma expression; directionality indicates up- or down-regulation. pGFWER = p-value with adjustments appropriate to a multiplexed interaction network. (20)

We next used the Pathways2Targets algorithm to identify potentially novel drug targets for BCNHL from the signaling pathway results (S6 File). We sorted the results so that drug targets present in multiple signaling pathways would be ranked higher (Table 6, S7 File). We predicted the most relevant existing FDA-approved drugs for other indications that could affect the lymphoma phenotype are Doxycycline, Ocriplasmin, and Collagenase. We also identified ATN-161 as a candidate drug, but it has only been tested in phase-two trials.

Table 6. Predicted BCNHL drugs based on signaling pathways.

	Drug Name	Drug ID	Significant Pathways Targeted	Is FDA Approved	Highest Clinical Trial Phase	Has Been Withdrawn
1	OCRIPLASMIN	CHEMBL2095222	13	TRUE	4	FALSE
2	ATN-161	CHEMBL4297456	10	FALSE	2	FALSE
3	DOXYCYCLINE	CHEMBL1200699	10	TRUE	4	FALSE
4	DOXYCYCLINE	CHEMBL1433	10	TRUE	4	FALSE
5	AS-1409	CHEMBL2109413	9	FALSE	1	FALSE
6	COLLAGENASE CLOSTRIDIUM HISTOLYTICUM	CHEMBL2108709	9	TRUE	4	FALSE
7	FIRATEGRAST	CHEMBL2104967	9	FALSE	2	FALSE
8	L19IL2	CHEMBL2109608	9	FALSE	3	FALSE
9	L19SIP 131I	CHEMBL2109412	9	FALSE	2	FALSE
10	L19TNFA	CHEMBL2109589	9	FALSE	2	FALSE
11	VOLOCIXIMAB	CHEMBL2108061	9	FALSE	3	FALSE
12	ABITUZUMAB	CHEMBL2109621	8	FALSE	2	FALSE
13	AL-78898A	CHEMBL4594457	8	FALSE	2	FALSE
1	CILENGITIDE	CHEMBL429876	8	FALSE	3	FALSE

4						
15	EPTIFIBATIDE	CHEMBL1174	8	TRUE	4	FALSE
16	ETARACIZUMAB	CHEMBL1743014	8	FALSE	2	FALSE
17	HUMAN C1-ESTERASE INHIBITOR	CHEMBL4297549	8	TRUE	4	FALSE
18	INTETUMUMAB	CHEMBL1743032	8	FALSE	2	FALSE
19	PEGCETACOPLAN	CHEMBL4298211	8	FALSE	3	FALSE

The top 19 drug predictions for BCNHL. Included are several drugs currently in use and others that are novel candidates.

Rather than solely rely on the significant differential expression data to determine biomarkers, we applied a more robust random forest machine learning method to predict biomarkers of BCNHLs. Specifically, the DEG statistics focus on identifying genes that have a large difference in expression between two states, while the random forest approach identifies genes that consistently change across disease vs. healthy samples. Consequently, the random forest approach identifies transcripts that are best capable of differentiating between disease and healthy states. The top three genes identified by our random forest analysis included YES1, FAM98B, and FERMT2 (Table 7, Figs 4A and 4B, S8 File). We then calculated the area under the curve for the receiver-operator characteristic curve, which showed that when the expression values from these three genes are combined they are 99.889% accurate at predicting whether the patient samples had BCNHL (Fig 4C).

Figure 4. Biomarker Prediction Yields Three-Gene Signature with 99% Predictive Ability.

A) Biomarkers ranked by mean decrease in Gini impurity and permutation values using random forest show YES1, FAM98B, and FERMT2 as the highest ranked predictive biomarkers (ranked by mean decrease of Gini impurity score). B) Random forest biomarker prediction for the top three genes in isolation. C) Receiver-operator characteristic curve using only YES1, FAM98B, and FERMT2 shows these three genes are 99.889% accurate at predicting BCNHL status (healthy or diseased).

Table 7. BCNHL biomarkers predicted from gene expression using machine learning

Gene Symbol	Mean Gini Decrease	edgeR Log_2 Fold Change	edgeR False Discovery Rate	Disease Status	Mean (Read Counts)	Standard Deviation (Read Counts)	Median (Read Counts)
YES1	0.77	2.38	$1.98x10^{-38}$	Lymphoma	1151.756	1246.946	629
				Healthy	38.87234	66.01043	11
FAM98B	0.68	1.58	$1.48x10^{-60}$	Lymphoma	1797.452	1174.797	1456
				Healthy	248.4202	954.1375	32
FERMT2	0.67	2.83	$1.46x10^{-38}$	Lymphoma	1246.993	1200.669	841
				Healthy	32.46809	73.10299	4

The top three genes identified by our random forest biomarker prediction are high-fidelity biomarkers of BCNHL due to their consistent and extreme upregulation across our 134 clinical BCNHL samples as compared to our 188 healthy B-cell samples. Presented above are statistics that capture the spread of transcriptional levels between BCNHL and healthy groups.

Discussion

The goal of this study was to collect publicly available RNA-seq data from GEO and process those data to find differentially expressed genes, pathways, splice variants, and biomarkers. We confirmed several biologically- and clinically relevant biomarkers and pathologic mechanisms that were identified previously, as well as novel entities. We found several key genes that are significantly differentially expressed in BCNHL including LUM and other SLRPs, complement protein components, and the supposed pseudogene AL512646.1. We confirmed that previously characterized biomarkers such as APOC1, VCAM1, CCL18, and CXCL9 are overexpressed in BCNHL, and that 320 genes including APOE, COL1A1, and COL27A1 had differentially expressed splice variants. We additionally found a BCNHL reliance on the upregulation of pathways associated with the extracellular matrix.

To our knowledge, this is the largest meta-analysis of human samples in the BCNHL field to-date. While some may be concerned that the signals from the individual subtypes of non-Hodgkin's B-cell lymphomas could drown one another out, we believe that including representative samples from multiple BCNHL subtypes augments the signal(s) that are shared among the represented subtypes and could aid in the identification of shared mechanistic insights with reduced bias. One potential limitation of our study was to only evaluate samples from the GEO database for

inclusion in our analysis. Our intentional focus on BCNHL excluded multiple myelomas, B-cell leukemias, or Hodgkin's B-cell lymphomas. Promising future directions may include mining additional public databases for similar data and potentially expanding the scope of any future meta-analysis to include all B-cell malignancies. In addition, it is possible that our focus on incorporating multiple publicly available datasets may have introduced potential biases in patient age, gender, or ethnicity.

Though there is evidence in the literature that directly associate BCNHL to some of our results (e.g. genes, splice variants, and pathways), some of our findings are novel to BCNHL. In cases where no previously published research indicates the relationship between BCNHL and our results, we will appeal to the Hallmarks of Cancer to investigate the relationship between our differentially expressed result and a distinct cancer system (4). We therefore ranked both the accuracy and confidence in our results by their relevance to BCNHL, followed by B-cell cancers in general, all blood cancers, and finally all cancers. We believe that identifying a possible mechanism for a gene that is associated with other cancers, and unresearched in BCNHL is still relevant. We expect that a subset of these findings will justify additional wet lab experimentation.

Differentially expressed genes suggest shared underlying mechanisms for lymphomas

LUM seems to play a role in the progression or non-progression of several different cancer types. Mahadevan *et al.* previously reported upregulated LUM in both T- and B-cell lymphomas, but offered no insights on potential mechanisms (21). A literature search of parallel systems revealed that in breast cancer, high stromal-cell expression of LUM adjacent to the tumor stalls tumor growth, and lowered stromal expression of LUM correlates with higher breast cancer mortality rates and increased severity (22). In melanoma, LUM in the extracellular matrix halts metastasis through direct interaction with alpha-2-beta-1 integrin (23). Both breast cancer and pancreatic

cancer cells have been documented to upregulate LUM, along with many other cancer types (19). Overall, LUM expression by cancer cells seems to correlate with more aggressive cancers and poorer patient outcomes. The massive LUM upregulation illustrated in our samples may be due to the fact that the BCNHL samples available on GEO were mostly from advanced or refractory cases of BCNHL. The prior finding that high LUM expression around tumors is protective against metastasis in several cancer subtypes indicates the potential for LUM as a cancer-stalling therapy.

Interestingly, a subset of the members in the SLRP protein family have been previously identified in B-cell Non-Hodgkin's lymphomas including DCN (24), BGN (24), ASPN (25), FMOD (26), LUM (21), PRELP (26), and TSKU (27). However, other members within the SLRP family have not been previously considered as lymphoma biomarkers or potential pathology-inducing molecules. Our novel finding is that the SLRPs ECM2, CHAD, PODN, and PODNL1 are differentially expressed in BCNHL. Proteoglycans have been shown to be associated with pro-cancer mechanisms in prostate, breast, colon, lung, ovary, mesothelium, pancreatic, lymphoma, and esophageal cancers (19). Our results show two upregulated pathways in BCNHL that were previously shown to be mechanistically intertwined with proteoglycans in cancer, which are the Focal Adhesion pathway (28) and the PI3K-Akt signaling pathway (29). Taken together, this may suggest a connection between previously established proteoglycan cancer mechanisms and B-cell non-Hodgkin's lymphomas. Additional work is still required to elucidate the role(s) that these entities play in BCNHL.

In the context of other cancers, increased expression of complement genes C1QA and C1QB at week 16 of mantle cell lymphoma treatment by Venetoclax and Ibrutinib was significantly associated with a worse prognosis (30), illustrating that C1QA and C1QB may be associated with resistance to cancer drugs. Jiang et al. showed via immunohistochemistry that C1QB localizes to the nuclei of gastric cancer cells (31). C1QB's nuclear localization suggests that C1QB may have

additional function(s). Upregulation of C1QA, C1QB, and C1QC in peripheral T-cell lymphoma (32) and upregulation of C1QC in Epstein-Barr Virus-positive diffuse large B-cell lymphoma (33) have been reported previously. In other in-vitro and in-vivo cancer models, the whole C1q protein has been shown to mediate metastasis, motility, growth and proliferation, and adhesion (34). Our results add to the growing body of work suggesting a potential alternate function of complement proteins in cancer that warrants further investigation.

In addition to our novel findings on differentially expressed genes, we were also able to detect statistically significant genes that were previously characterized in at least one subtype of BCNHL. The first of these proteins is Apolipoprotein C1 (APOC1), which we observed to be upregulated in BCNHL. APOC1 is one of three genes whose expression levels are predictive of diffuse large B-cell lymphoma severity (35), and it is also upregulated in late stage lung cancers as compared to early stage lung cancers (36). This suggests that APOC1 may be contributing to cancer pathology across diverse cancers in multiple cell types.

Our observation that C-C motif chemokine ligand 18 (CCL18), which has a well-recognized role in lymphoma, was upregulated in our BCNHL analysis is relevant since this gene assists large B-cell lymphoma in cell proliferation, the NF-Kappa-B pathway, and the PI3K-AKT pathway (37). Its upregulation in macrophages and dendritic cells from cutaneous T-cell lymphoma lesions was associated with a negative prognosis (38).

Our finding C-X-C motif chemokine ligand 9 (CXCL9) to be significantly upregulated in our analysis of B-cells is interesting since this gene has been shown to promote the progression of diffuse large B-cell lymphoma by halting degradation of beta-catenin (CTNNB1) and upregulating its initial expression (39). Our findings support this proposed mechanism with CTNNB1 being upregulated in lymphoma ($\log_2$FC = 1.1, FDR = 1.54×10^{-33}), while other elements of the CTNNB1 “destruction complex” were mostly downregulated. Specifically, several of the known

components of the destruction complex that were detected in our analysis include APC (log_2FC = -0.755, FDR = 3.51×10^{-11}), GSK3B (log_2FC = -0.692, FDR = 2.62×10^{-3}), CSNK1A1 (not significant), AXIN1 (log_2FC = 0.533, FDR = 3.96×10^{-10}), BTRC (not significant), and FBW11 (log_2FC = -0.692, FDR = 5.60×10^{-20}).

We identified several other genes of that may be relevant to pathogenesis. Small but significant upregulation of AXIN1 is of interest for additional investigation due to its ties to CXCL9, and is not known to have multiple heterogenous functions (40). AXIN1 regulates the Wnt and JNK signaling pathways (41), and it regulates the Wnt pathway by degrading CTNNB1 (39). If CTNNB1 isn't degraded by AXIN1, CTNNB1 translocates to the nucleus and interacts with LEF1, which we found to be significantly upregulated, and TCF7 (not significant in this study), causing transcription of Wnt pathway target genes to occur (42,43). Wnt helps to regulate cell cycle and contributes to the increased growth rate of many cancer types (44). AXIN1 activates the JNK signaling pathway by binding to MAP3K1, which we found to be significantly downregulated, or to MAP3K4, which was significantly upregulated (45). Since CTNNB1 has been shown to contribute to apoptosis resistance in multiple myeloma cells (46), it is possible that the inability to stop the destruction of CTNNB1 in lymphoma may share a similar mechanism.

Finally, VCAM1 upregulation is associated with a poor prognosis for patients with non-Hodgkin's lymphomas, and VCAM1 is under investigation as a potential serum biomarker for assessing disease progression (47). Adhesion molecules such as VCAM1 promote cancer metastasis, or in the case of blood cancers, extravasation, by allowing cancer cells to exit the bloodstream and integrate with healthy tissues throughout the body (48).

Splice variants suggest relevance to lymphomas

To better understand the contribution of differentially expressed splice variants to disease, we examined the highest-ranked DRIMseq results. This algorithm calculates statistical significance

based on the number of reads mapped to exons that are present in each splice variant. Our observation that Apolipoprotein E (APOE) was the highest-ranking splice variant result validates previous findings that associate this gene with pancreatic cancer pathology (49). In addition, pediatric patients with malignant lymphoma and acute lymphoblastic leukemia who express isoforms E3 and E4 of APOE are at higher risk of developing extreme hypertriglyceridemia (50). Though little research has been done concerning the mechanisms of APOE in BCNHL, we believe that APOE may be contributing to disease by participating in the Regulation of Insulin-like Growth Factor (IGF) activity by Insulin-like Growth Factor Binding Protein (IGFBP) pathway, which is we found to be a significantly modulated pathway that includes APOE. The significance of APOC1 as a DEG in BCNHL, paired with the evidence of significant APOE splice variants suggest that apolipoproteins may be useful targets for future BCNHL treatments.

Our observation of Collagen type I alpha 1 chain (COL1A1) as a highly ranked splice variant result is novel to the best of our knowledge. However, the literature indicates that the COLA1A-014 transcript regulates the CXCL12-CXCR4 axis in gastric cancer, leading to tumor progression (46). In addition to displaying significant differences in splice variant expression, we also found COL1A1 to be significantly upregulated in BCNHL. COL1A1 has previously been reported to be upregulated in peripheral T-cell lymphoma (21). In Hodgkin's lymphoma, COL1A1 overexpression is associated with epigenetic silencing of the RNA demethylase ALKBH3 and reduced survival (51). COL1A1 is a member of several of our significant upregulated pathways involving the extracellular matrix (ECM-receptor interaction, Focal adhesion, Extracellular matrix organization, and Collagen formation). This involvement in extracellular matrix-related pathways strengthens the case that the mechanism of COL1A1 may involve tumor cell interaction with its outer environment.

Collagen type XXVII alpha 1 chain (COL27A1) having significant changes among its expressed splice variants in BCNHL is interesting since it was recently reported as being overexpressed in

adenoid cystic carcinoma (52). Like COL1A1, COL27A1 is a member of the upregulated Extracellular matrix organization and Collagen formation pathways, suggesting that COL27A1 could play a role in BCNHL extravasation.

Extracellular matrix-related pathways may contribute to disease

Our signaling pathway enrichment analysis broadened the scope of our analysis and interpretation. Many of our findings supported an interesting reliance of BCNHL on pathways associated with the extracellular matrix. Recent research has suggested the importance of extracellular matrix components in reactivating quiescent cancer cells through the β1-integrin signaling pathway (53). It would follow that interaction with extracellular matrix components also plays a role in regulating cancer cells. To our knowledge, no studies have reported the integrin signaling pathway to be activated in BCNHL, though it has been reported as activated in the closely-related cancer NK/T-cell lymphoma (21). The activation of these pathways suggests that malignant BCNHL cells may have an advantage by interacting with the extracellular matrix. Such interactions with the extracellular matrix are typically considered to be an important part of metastasis (48). We found this result to be interesting since lymphomas are liquid tumors, unbound by extracellular matrix. This upregulation of pathways allowing interaction with the extracellular matrix may suggest that BCNHL could be invading non-lymphatic and/or non-circulatory tissues.

The trend of extracellular matrix interaction is also seen in the DEG results, adding support to the idea that interaction with the extracellular matrix is important for BCNHL growth and survival. Additionally, COL1A1 and COL27A1, which are members of extracellular matrix-related pathways, are two of the genes with the most significantly differential expression of splice variants.

Drug prediction algorithm returned both tested and novel candidates

Of our top drug results, doxycycline is currently in use for ocular B-cell lymphomas (54,55). It is additionally under investigation for diffuse large B-cell lymphoma; recent work found doxycycline suppresses diffuse large B-cell lymphoma growth *in vitro* and *in vivo* via CSN5 inhibition (56). ATN-161 is a novel drug candidate for BCNHL. Though it is only in phase two of clinical trials, it has been a successful drug against refractory solid tumors, making it a promising drug candidate for other susceptible malignancies (57). ATN-161 suppresses cancer via integrin beta1 alpha5 antagonism, disabling invasion and metastasis (58). Ocriplasmin reverses vitreomacular adhesion via interaction with fibronectin and laminin (59). Though ocriplasmin has never been used in cancer before, it may be a promising drug candidate due to its ability to modulate adhesion. Collagenase clostridium histolyticum is under investigation for treating collagen-rich uterine fibroids and was successful at reducing the stiffness of the tumors (60).

Machine learning predicts novel biomarkers of BCNHL

YES1, FERMT2, and FAM98B are novel biomarkers not previously associated with BCNHL. However, each has well-documented cancer associations. YES1 is a tyrosine kinase which regulates cell cycle and apoptosis *in vitro* and cell growth *in vivo* of tumors with YES1 amplification (61). YES1 has been previously identified as a biomarker for non-small cell lung cancer and esophageal adenocarcinoma (62,63) and may be a potential membrane biomarker. YES1 can anchor to the inner membrane with help from peptide SMIM30 (64), but whether it can flip to the outer leaflet has not been investigated. The role of YES1 in BCNHL pathogenesis also needs additional investigation. FERMT2 has previously been pinpointed as a biomarker for other cancers previously including non-small cell lung cancer and prostate cancer (65,66), but not for BCNHL. FERMT2 stabilizes CTNNB1, which is a well-documented activator of oncogene transcription, and is implicated in Wnt pathway regulation (67). Additionally, FERMT2 enhances

integrin signaling and mediates migration, invasion, and focal adhesion (68,69). Though FAM98B has been shown to play an important role in the development of multiple cancers, it has not previously been identified as a biomarker for any cancer. FAM98B is an arginine methyltransferase, is utilized in tumorigenesis, and works in tandem with DDX1, a pan-cancer marker, in RNA metabolism/processing (70,71). Like YES1 and FERMT2, FAM98B has not been previously identified as a biomarker for BCNHL. These three genes have substantial diagnostic potential as a liquid biopsy that could be generalizable across B-cell non-Hodgkin's lymphoma subtypes. Further validation is needed to determine whether these are suitable biomarkers for diagnostic or screening application.

In summary, our meta-analysis identified many significant DEGs and pathways that play a role in B-cell non-Hodgkin's lymphomas. Our findings confirm results of previous BCNHL research, indicating that the statistical analyses applied within our computational workflow pipeline are effective at accurately identifying statistically significant genes, splice variants, and pathways with clinical and pathological relevance. Additionally, several of our results are novel, which need additional validation in future experiments. It is likely that at least some of these novel findings were detected due to the ability of our meta-analysis to reduce the statistical "noise" produced by outliers from individual studies and increase the biologically-relevant signal. Specifically, our findings suggest that LUM and 10 other small leucine-rich proteoglycans are significantly differentially expressed in BCNHL, that AL512646.1 is not a pseudo-gene, that APOE, COL1A1, and COL27a1 have significant differentially expressed splice variants in BCNHL, and that BCNHL is strongly reliant on the overexpression of extracellular matrix-associated pathways. The predominant drug prediction results nearly universally targeted extracellular matrix-associated mechanisms, and has yielded several promising new potential drug candidates including ocriplasmin and ATN-161. Our random forest biomarker discovery pinpointed three novel biomarker genes not previously associated with BCNHL, YES1, FERMT2, and FAM98B, which

show high fidelity in predicting lymphoma presence based on transcriptional levels. These findings shed additional light on the underlying intracellular mechanisms of BCNHL and could be used in the development of improved diagnostics and therapeutics to further improve human health.

Methods

Collecting samples

RNA-sequencing samples were acquired from the National Center for Biotechnology Information (NCBI) Gene Expression Omnibus (GEO) database using the search term, “b-cell lymphoma” to find B-cell non-Hodgkin’s lymphoma samples and healthy B-cell controls. The automatic GEO filters “Homo sapiens” and “high-throughput RNA-sequencing” were applied. Cell lines, formalin-fixed paraffin-embedded tissues, gene expression microarray experiments, single-cell (10X) RNA-sequencing experiments, xenografts, samples known to be infected with EBV and KSHV, and samples which contained more diverse cell types (i.e., whole blood, lymph node, PBMCs, brain, etc.) were manually excluded. All samples that had one or more of these disqualifying attributes were excluded from the dataset prior to analysis, which may have included only a subset of samples from any individual study in the meta-analysis. Multiple myeloma, leukemia, and Hodgkin’s lymphoma samples were intentionally excluded in favor of focusing on B-cell non-Hodgkin’s lymphomas. Records were accepted or rejected based on the standardized exclusion criteria detailed above by our team. To avoid inclusion bias, any sample that could not be excluded by the standardized exclusion criteria was included in the study. While a subset of the healthy control samples was obtained from the same RNA sequencing projects as the BCNHL samples, others were obtained from three unrelated B-cell datasets with healthy controls to create roughly equivalent-sized BCNHL and healthy groups. Final dataset assembly from GEO concluded on October 22, 2020, resulting in a dataset of 322 samples (134 BCNHL samples and

188 healthy B-cell controls) from ten studies (7–18). The raw data for these experiments were previously collected by the data providers and conform to the appropriate ethical oversight to protect patient autonomy and patient identity. All 10 primary RNA-sequencing datasets from which samples were gathered for our lymphoma meta-analysis have been published in the peer-reviewed literature, increasing overall confidence that each dataset has acceptable quality (Table 1, Fig 1).

Preprocessing of RNA-sequencing data

Following the manual curation of the RNA-seq samples, the fastq files were pre-processed as previously described (72). In brief, fastq files containing RNA-sequencing data were downloaded from the Sequence Read Archive (SRA) using the sratools software package. The fastq files, the associated metadata file, and a configuration file for each dataset were then generated and used as input to the Automated Reproducible MOdular Workflow for Preprocessing and Differential Analysis of RNA-seq Data (ARMOR) workflow (73). A configuration file was used by ARMOR to appropriately set up a python-based Snakemake workflow (74). In the ARMOR workflow, adapters and poor-quality regions of reads were trimmed with TrimGalore! (75), quality control metrics were calculated with FastQC (76), reads were mapped to the human GRCh38 transcriptome and total gene transcripts quantified with Salmon (77), significant differential gene expression was calculated using a negative binomial distribution implemented in edgeR (78), Gene Ontology enrichment was performed against terms from the MSigDB (79) while adjusting for inter-gene correlation using the Camera algorithm (80), and significant splice variants were predicted with DRIMseq (81). The significant differentially expressed genes from the ARMOR workflow were then used as input to the signaling pathway impact analysis (SPIA) algorithm to enrich differentially expressed genes against intracellular signaling pathways from five databases including KEGG, Panther, BioCarta, Reactome, and NCI (20,82–85). Differentially expressed genes and splice variants calculated by ARMOR and DRIMSeq were evaluated by the effect

551 measures log2 fold change and likelihood ratio respectively. Confidence in results was
552 accomplished using false discovery-rate adjusted p-values.
553

554 Additional analysis and visualization of differentially expressed
555 genes and gene ontologies

556 The PRISMA flowchart template was used to generate figure one consistent with transparent
557 reporting of meta-analysis generation and results (86).
558

559 The R package ggplot was used to construct the Fig 2 volcano plot from using FDRs and log2
560 fold change values for each gene from the edgeR output (87).
561

562 The KEGG ontology was extracted from the Brite Hierarchy using existing code (82). Genes
563 included in the Brite Hierarchy were then computationally matched to their corresponding edgeR
564 $\log_2$ fold change values. A statistical enrichment of the KEGG gene ontologies was performed
565 using the R package bc3net (88) prior to visualizing the bc3net enrichment results with the R
566 package Treemap in Fig 3 (89).
567

568 Biomarker prediction using differentially expressed gene data

569 Salmon-derived transcript counts were organized into a tabular format and samples were
570 randomly assigned to either the testing set (30%) or the training set (70%). The R package
571 randomForest was used to run a supervised classification analysis to determine biomarkers (90).
572 The initial results from the whole transcriptome were then reduced to the 3, 5, and 10 best-
573 scoring transcriptional biomarkers, based on the mean Gini impurity decrease values for each of
574 the features. These values were then sorted by size to determine the transcribed genes from the
575 original dataset with the largest association. The area under the curve (AUC) was calculated from

the receiver operator characteristic curves that were generated for each set of random forest results to determine the efficacy of the selected biomarkers for disease prediction.

Drug prediction using differentially modulated pathways

Drug prediction was conducted by running the significantly modulated pathways file that was generated by SPIA file through Pathways2Targets2.R algorithm (91). To summarize drug findings, the Pathways2Targets output was processed using a custom R script most_common_treatments_2021_09_19.R (92).

Other information

This meta-analysis was not registered. The review protocol was not prepared separately but is described in detail in the methods section. This meta-analysis received no specific financial support and was supported by general funding from Brigham Young University. Brigham Young University played no role in the ideation, synthesis, or analysis of this transcriptomic meta-analysis. The authors each declare that they have no competing interests. All raw data analyzed in this study can be found in NCBI's GEO. Analytical codes can be found as cited in materials and methods. All processed data are available in the supplementary materials or at DOI: 10.5281/zenodo.4757764.

Acknowledgments

We thank the high-performance computing resources hosted by the BYU Research Computing Center. We also gratefully acknowledge those who generated, provided, and submitted the original data.

References

1. Global Burden of Disease Cancer Collaboration. Global, Regional, and National Cancer Incidence, Mortality, Years of Life Lost, Years Lived With Disability, and Disability-Adjusted Life-Years for 29 Cancer Groups, 1990 to 2016: A Systematic Analysis for the Global Burden of Disease Study. JAMA Oncology. 2018 Nov 1;4(11):1553–68.

2. Shankland KR, Armitage JO, Hancock BW. Non-Hodgkin lymphoma. The Lancet. 2012 Sep 1;380(9844):848–57.

3. Küppers R. Mechanisms of B-cell lymphoma pathogenesis. Nat Rev Cancer. 2005 Apr;5(4):251–62.

4. Hanahan D, Weinberg RA. The hallmarks of cancer. Cell. 2000 Jan 7;100(1):57–70.

5. Fouad YA, Aanei C. Revisiting the hallmarks of cancer. Am J Cancer Res. 2017;7(5):1016–36.

6. Ochoa D, Hercules A, Carmona M, Suveges D, Gonzalez-Uriarte A, Malangone C, et al. Open Targets Platform: supporting systematic drug-target identification and prioritisation. Nucleic Acids Res. 2021 Jan 8;49(D1):D1302–10.

7. Faramand R, Jain M, Staedtke V, Kotani H, Bai R, Reid K, et al. Tumor Microenvironment Composition and Severe Cytokine Release Syndrome (CRS) Influence Toxicity in Patients with Large B-Cell Lymphoma Treated with Axicabtagene Ciloleucel. Clin Cancer Res. 2020 Sep 15;26(18):4823–31.

8. Li M, Chiang YL, Lyssiotis CA, Teater MR, Hong JY, Shen H, et al. Non-oncogene Addiction to SIRT3 Plays a Critical Role in Lymphomagenesis. Cancer Cell. 2019 Jun 10;35(6):916-931.e9.

9. Porpaczy E, Tripolt S, Hoelbl-Kovacic A, Gisslinger B, Bago-Horvath Z, Casanova-Hevia E, et al. Aggressive B-cell lymphomas in patients with myelofibrosis receiving JAK1/2 inhibitor therapy. Blood. 2018 Aug 16;132(7):694–706.

10. Teater M, Dominguez PM, Redmond D, Chen Z, Ennishi D, Scott DW, et al. AICDA drives epigenetic heterogeneity and accelerates germinal center-derived lymphomagenesis. Nat Commun. 2018 Jan 15;9(1):222.

11. Raju S, Kretzmer LZ, Koues OI, Payton JE, Oltz EM, Cashen A, et al. NKG2D-NKG2D Ligand Interaction Inhibits the Outgrowth of Naturally Arising Low-Grade B Cell Lymphoma In Vivo. J Immunol. 2016 Jun 1;196(11):4805–13.

12. Koues OI, Kowalewski RA, Chang LW, Pyfrom SC, Schmidt JA, Luo H, et al. Enhancer sequence variants and transcription-factor deregulation synergize to construct pathogenic regulatory circuits in B-cell lymphoma. Immunity. 2015 Jan 20;42(1):186–98.

13. Rouhigharabaei L, Finalet Ferreiro J, Tousseyn T, van der Krogt JA, Put N, Haralambieva E, et al. Non-IG aberrations of FOXP1 in B-cell malignancies lead to an aberrant expression of N-truncated isoforms of FOXP1. PLoS One. 2014;9(1):e85851.

14. Béguelin W, Popovic R, Teater M, Jiang Y, Bunting KL, Rosen M, et al. EZH2 is required for germinal center formation and somatic EZH2 mutations promote lymphoid transformation. Cancer Cell. 2013 May 13;23(5):677–92.

15. Verma A, Jiang Y, Du W, Fairchild L, Melnick A, Elemento O. Transcriptome sequencing reveals thousands of novel long non-coding RNAs in B cell lymphoma. Genome Med. 2015 Nov 1;7:110.

16. Jenks SA, Cashman KS, Zumaquero E, Marigorta UM, Patel AV, Wang X, et al. Distinct Effector B Cells Induced by Unregulated Toll-like Receptor 7 Contribute to Pathogenic Responses in Systemic Lupus Erythematosus. Immunity. 2018 Oct 16;49(4):725-739.e6.

17. Scharer CD, Blalock EL, Mi T, Barwick BG, Jenks SA, Deguchi T, et al. Epigenetic programming underpins B cell dysfunction in human SLE. Nat Immunol. 2019 Aug;20(8):1071–82.

18. Wang S, Wang J, Kumar V, Karnell JL, Naiman B, Gross PS, et al. IL-21 drives expansion and plasma cell differentiation of autoreactive CD11chiT-bet+ B cells in SLE. Nat Commun. 2018 May 1;9(1):1758.

19. Appunni S, Anand V, Khandelwal M, Gupta N, Rubens M, Sharma A. Small Leucine Rich Proteoglycans (decorin, biglycan and lumican) in cancer. Clin Chim Acta. 2019 Apr;491:1–7.

20. Tarca AL, Draghici S, Khatri P, Hassan SS, Mittal P, Kim JS, et al. A novel signaling pathway impact analysis. Bioinformatics. 2009 Jan 1;25(1):75–82.

21. Mahadevan D, Spier C, Croce KD, Miller S, George B, Riley CJ, et al. Gene Expression Profiling of Peripheral T-Cell Lymphoma (PTCL, NOS) and Comparison to Diffuse Large B-Cell Lymphoma (DLBCL). Blood. 2004 Nov 16;104(11):2277–2277.

22. Troup S, Njue C, Kliewer EV, Parisien M, Roskelley C, Chakravarti S, et al. Reduced Expression of the Small Leucine-rich Proteoglycans, Lumican, and Decorin Is Associated with Poor Outcome in Node-negative Invasive Breast Cancer. Clin Cancer Res. 2003 Jan 1;9(1):207–14.

23. Brézillon S, Pietraszek K, Maquart FX, Wegrowski Y. Lumican effects in the control of tumour progression and their links with metalloproteinases and integrins. FEBS J. 2013 May;280(10):2369–81.

24. Kotlov N, Bagaev A, Revuelta MV, Phillip JM, Cacciapuoti MT, Antysheva Z, et al. Clinical and Biological Subtypes of B-cell Lymphoma Revealed by Microenvironmental Signatures. Cancer Discov. 2021 Jun 1;11(6):1468–89.

25. Sarkozy C, Chong L, Takata K, Chavez EA, Miyata-Takata T, Duns G, et al. Gene expression profiling of gray zone lymphoma. Blood Advances. 2020 Jun 9;4(11):2523–35.

26. Mikaelsson E, Jeddi-Tehrani M, Ã–Sterborg A, Shokri F, Rabbani H, Mellstedt H. Small Leucine Rich Proteoglycans as Novel Tumor Markers In Chronic Lymphocytic Leukemia. Blood. 2010 Nov 19;116(21):694.

27. Huang H, Zhang D, Fu J, Zhao L, Li D, Sun H, et al. Tsukushi is a novel prognostic biomarker and correlates with tumor-infiltrating B cells in non-small cell lung cancer. Aging (Albany NY). 2021 Jan 10;13(3):4428–51.

28. Munesue S, Kusano Y, Oguri K, Itano N, Yoshitomi Y, Nakanishi H, et al. The role of syndecan-2 in regulation of actin-cytoskeletal organization of Lewis lung carcinoma-derived metastatic clones. Biochem J. 2002 Apr 15;363(Pt 2):201–9.

29. Mahtouk K, Tjin EPM, Spaargaren M, Pals ST. The HGF/MET pathway as target for the treatment of multiple myeloma and B-cell lymphomas. Biochim Biophys Acta. 2010 Dec;1806(2):208–19.

30. Davis J, Handunnetti SM, Sharpe C, Turner G, Anderson MA, Roberts AW, et al. Long Term Responses to Venetoclax and Ibrutinib in Mantle Cell Lymphoma Are Associated with Immunological Recovery and Prognostic Changes in Inflammatory Biomarkers. Blood. 2019 Nov 13;134(Supplement_1):2791–2791.

31. Jiang J, Ding Y, Wu M, Lyu X, Wang H, Chen Y, et al. Identification of TYROBP and C1QB as Two Novel Key Genes With Prognostic Value in Gastric Cancer by Network Analysis. Front Oncol. 2020;10:1765.

32. Gao HX, Wang MB, Li SJ, Niu J, Xue J, Li J, et al. Identification of Hub Genes and Key Pathways Associated with Peripheral T-cell Lymphoma. Curr Med Sci. 2020 Oct;40(5):885–99.

33. Yoon H, Park S, Ju H, Ha SY, Sohn I, Jo J, et al. Integrated copy number and gene expression profiling analysis of Epstein-Barr virus-positive diffuse large B-cell lymphoma. Genes Chromosomes Cancer. 2015 Jun;54(6):383–96.

34. Bulla R, Tripodo C, Rami D, Ling GS, Agostinis C, Guarnotta C, et al. C1q acts in the tumour microenvironment as a cancer-promoting factor independently of complement activation. Nat Commun. 2016 Feb 1;7(1):10346.

35. Zamani-Ahmadmahmudi M, Nassiri SM. Development of a Reproducible Prognostic Gene Signature to Predict the Clinical Outcome in Patients with Diffuse Large B-Cell Lymphoma. Sci Rep. 2019 Aug 21;9(1):12198.

36. Ko HL, Wang YS, Fong WL, Chi MS, Chi KH, Kao SJ. Apolipoprotein C1 (APOC1) as a novel diagnostic and prognostic biomarker for lung cancer: A marker phase I trial. Thorac Cancer. 2014 Nov;5(6):500–8.

706 37. Zhou Q, Huang L, Gu Y, Lu H, Feng Z. The expression of CCL18 in diffuse large B cell
707 lymphoma and its mechanism research. Cancer Biomark. 2018;21(4):925–34.

708 38. Miyagaki T, Sugaya M, Suga H, Ohmatsu H, Fujita H, Asano Y, et al. Increased CCL18
709 expression in patients with cutaneous T-cell lymphoma: association with disease severity
710 and prognosis. J Eur Acad Dermatol Venereol. 2013 Jan;27(1):e60-67.

711 39. Ruiduo C, Ying D, Qiwei W. CXCL9 promotes the progression of diffuse large B-cell
712 lymphoma through up-regulating β-catenin. Biomedicine & Pharmacotherapy. 2018 Nov
713 1;107:689–95.

714 40. Mani M, Chen C, Amblee V, Liu H, Mathur T, Zwicke G, et al. MoonProt: a database for
715 proteins that are known to moonlight. Nucleic Acids Research. 2015 Jan 28;43(D1):D277–
716 82.

717 41. Kusano S, Raab-Traub N. I-mfa domain proteins interact with Axin and affect its regulation
718 of the Wnt and c-Jun N-terminal kinase signaling pathways. Mol Cell Biol. 2002
719 Sep;22(18):6393–405.

720 42. Bienz M. TCF: transcriptional activator or repressor? Current Opinion in Cell Biology. 1998
721 Jun 1;10(3):366–72.

722 43. Escobar G, Mangani D, Anderson AC. T cell factor 1: A master regulator of the T cell
723 response in disease. Sci Immunol. 2020 Nov 6;5(53):eabb9726.

724 44. Bugter JM, Fenderico N, Maurice MM. Mutations and mechanisms of WNT pathway
725 tumour suppressors in cancer. Nat Rev Cancer. 2021 Jan;21(1):5–21.

726 45. Luo W, Ng WW, Jin LH, Ye Z, Han J, Lin SC. Axin Utilizes Distinct Regions for Competitive
727 MEKK1 and MEKK4 Binding and JNK Activation *. Journal of Biological Chemistry. 2003 Sep
728 26;278(39):37451–8.

729 46. Su N, Wang P, Li Y. Role of Wnt/β-catenin pathway in inducing autophagy and apoptosis in
730 multiple myeloma cells. Oncol Lett. 2016 Dec;12(6):4623–9.

731 47. Shah N, Cabanillas F, McIntyre B, Feng L, McLaughlin P, Rodriguez MA, et al. Prognostic
732 value of serum CD44, intercellular adhesion molecule-1 and vascular cell adhesion
733 molecule-1 levels in patients with indolent non-Hodgkin lymphomas. Leuk Lymphoma.
734 2012 Jan;53(1):50–6.

735 48. Zetter BR. Adhesion molecules in tumor metastasis. Semin Cancer Biol. 1993 Aug;4(4):219–
736 29.

737 49. Omenn GS, Yocum AK, Menon R. Alternative splice variants, a new class of protein cancer
738 biomarker candidates: findings in pancreatic cancer and breast cancer with systems
739 biology implications. Dis Markers. 2010;28(4):241–51.

50. Tozuka M, Yamauchi K, Hidaka H, Nakabayashi T, Okumura N, Katsuyama T. Characterization of hypertriglyceridemia induced by L-asparaginase therapy for acute lymphoblastic leukemia and malignant lymphoma. Ann Clin Lab Sci. 1997 Sep 1;27(5):351–7.

51. Esteve-Puig R, Climent F, Piñeyro D, Domingo-Domènech E, Davalos V, Encuentra M, et al. Epigenetic loss of m1A RNA demethylase ALKBH3 in Hodgkin lymphoma targets collagen, conferring poor clinical outcome. Blood. 2021 Feb 18;137(7):994–9.

52. Arolt C, Meyer M, Hoffmann F, Wagener-Ryczek S, Schwarz D, Nachtsheim L, et al. Expression Profiling of Extracellular Matrix Genes Reveals Global and Entity-Specific Characteristics in Adenoid Cystic, Mucoepidermoid and Salivary Duct Carcinomas. Cancers. 2020 Sep;12(9):2466.

53. Barkan D, El Touny LH, Michalowski AM, Smith JA, Chu I, Davis AS, et al. Metastatic growth from dormant cells induced by a col-I-enriched fibrotic environment. Cancer Res. 2010 Jul 15;70(14):5706–16.

54. Kim TM, Kim KH, Lee MJ, Jeon YK, Lee SH, Kim DW, et al. First-line therapy with doxycycline in ocular adnexal mucosa-associated lymphoid tissue lymphoma: A retrospective analysis of clinical predictors. Cancer Science. 2010;101(5):1199–203.

55. Han JJ, Kim TM, Jeon YK, Kim MK, Khwarg SI, Kim CW, et al. Long-term outcomes of first-line treatment with doxycycline in patients with previously untreated ocular adnexal marginal zone B cell lymphoma. Ann Hematol. 2015 Apr 1;94(4):575–81.

56. Pulvino M, Chen L, Oleksyn D, Li J, Compitello G, Rossi R, et al. Inhibition of COP9-signalosome (CSN) deneddylating activity and tumor growth of diffuse large B-cell lymphomas by doxycycline. Oncotarget. 2015 Jun 4;6(17):14796–813.

57. Cianfrocca ME, Kimmel KA, Gallo J, Cardoso T, Brown MM, Hudes G, et al. Phase 1 trial of the antiangiogenic peptide ATN-161 (Ac-PHSCN-NH2), a beta integrin antagonist, in patients with solid tumours. Br J Cancer. 2006 Jun;94(11):1621–6.

58. Barkan D, Chambers AF. β1-Integrin: A Potential Therapeutic Target in the Battle against Cancer Recurrence. Clinical Cancer Research. 2011 Nov 30;17(23):7219–23.

59. Baldo BA. Enzymes Approved for Human Therapy: Indications, Mechanisms and Adverse Effects. BioDrugs. 2015 Feb 1;29(1):31–55.

60. Jayes FL, Liu B, Moutos FT, Kuchibhatla M, Guilak F, Leppert PC. Loss of stiffness in collagen-rich uterine fibroids after digestion with purified collagenase Clostridium histolyticum. American Journal of Obstetrics and Gynecology. 2016 Nov 1;215(5):596.e1-596.e8.

61. Hamanaka N, Nakanishi Y, Mizuno T, Horiguchi-Takei K, Akiyama N, Tanimura H, et al. YES1 Is a Targetable Oncogene in Cancers Harboring YES1 Gene Amplification. Cancer Research. 2019 Nov 15;79(22):5734–45.

62. Garmendia I, Pajares MJ, Hermida-Prado F, Ajona D, Bértolo C, Sainz C, et al. YES1 Drives Lung Cancer Growth and Progression and Predicts Sensitivity to Dasatinib. Am J Respir Crit Care Med. 2019 Oct;200(7):888–99.

63. Liu Z, Jiang F, Tian G, Wang S, Sato F, Meltzer SJ, et al. Sparse Logistic Regression with Lp Penalty for Biomarker Identification. Statistical Applications in Genetics and Molecular Biology [Internet]. 2007 Feb 10 [cited 2022 Apr 16];6(1). Available from: http://www.degruyter.com/document/doi/10.2202/1544-6115.1248/html

64. Pang Y, Liu Z, Han H, Wang B, Li W, Mao C, et al. Peptide SMIM30 promotes HCC development by inducing SRC/YES1 membrane anchoring and MAPK pathway activation. Journal of Hepatology. 2020 Nov 1;73(5):1155–69.

65. Sun W, Guo J, Cheng Z, Zhang Y, Gao Y. Identification of the Dysregulated Pathways and Key Gene in Prostate Cancer by Transcriptome Analysis and Cell Biology Experiments [Internet]. In Review; 2022 Jan [cited 2022 Apr 16]. Available from: https://www.researchsquare.com/article/rs-1122595/v1

66. Su X, Liu N, Wu W, Zhu Z, Xu Y, He F, et al. Comprehensive analysis of prognostic value and immune infiltration of kindlin family members in non-small cell lung cancer. BMC Med Genomics. 2021 May 2;14(1):119.

67. Yu Y, Wu J, Wang Y, Zhao T, Ma B, Liu Y, et al. Kindlin 2 forms a transcriptional complex with β-catenin and TCF4 to enhance Wnt signalling. EMBO Rep. 2012 Aug;13(8):750–8.

68. Kawamura E, Hamilton GB, Miskiewicz EI, MacPhee DJ. Fermitin family homolog-2 (FERMT2) is highly expressed in human placental villi and modulates trophoblast invasion. BMC Developmental Biology. 2018 Nov 1;18(1):19.

69. Yasuda-Yamahara M, Rogg M, Frimmel J, Trachte P, Helmstaedter M, Schroder P, et al. FERMT2 links cortical actin structures, plasma membrane tension and focal adhesion function to stabilize podocyte morphology. Matrix Biology. 2018 Aug 1;68–69:263–79.

70. Akter KA, Mansour MA, Hyodo T, Senga T. FAM98A associates with DDX1-C14orf166-FAM98B in a novel complex involved in colorectal cancer progression. Int J Biochem Cell Biol. 2017 Mar;84:1–13.

71. Gao B, Li X, Li S, Wang S, Wu J, Li J. Pan-cancer analysis identifies RNA helicase DDX1 as a prognostic marker. Phenomics. 2022 Feb 1;2(1):33–49.

72. Rapier-Sharman N, Krapohl J, Beausoleil EJ, Gifford KTL, Hinatsu BR, Hoffmann CS, et al. Preprocessing of Public RNA-Sequencing Datasets to Facilitate Downstream Analyses of Human Diseases. Data. 2021 Jul;6(7):75.

73. Orjuela S, Huang R, Hembach KM, Robinson MD, Soneson C. ARMOR: An Automated Reproducible MOdular Workflow for Preprocessing and Differential Analysis of RNA-seq Data. G3 (Bethesda). 2019 Jul 9;9(7):2089–96.

74. Köster J, Rahmann S. Snakemake--a scalable bioinformatics workflow engine. Bioinformatics. 2012 Oct 1;28(19):2520–2.

75. Babraham Bioinformatics - Trim Galore! [Internet]. [cited 2021 Jun 7]. Available from: https://www.bioinformatics.babraham.ac.uk/projects/trim_galore/

76. Babraham Bioinformatics - FastQC A Quality Control tool for High Throughput Sequence Data [Internet]. [cited 2021 Jun 7]. Available from: https://www.bioinformatics.babraham.ac.uk/projects/fastqc/

77. Patro R, Duggal G, Love MI, Irizarry RA, Kingsford C. Salmon provides fast and bias-aware quantification of transcript expression. Nat Methods. 2017 Apr;14(4):417–9.

78. Robinson MD, McCarthy DJ, Smyth GK. edgeR: a Bioconductor package for differential expression analysis of digital gene expression data. Bioinformatics. 2010 Jan 1;26(1):139–40.

79. Liberzon A, Subramanian A, Pinchback R, Thorvaldsdóttir H, Tamayo P, Mesirov JP. Molecular signatures database (MSigDB) 3.0. Bioinformatics. 2011 Jun 15;27(12):1739–40.

80. Wu D, Smyth GK. Camera: a competitive gene set test accounting for inter-gene correlation. Nucleic Acids Res. 2012 Sep 1;40(17):e133.

81. Nowicka M, Robinson MD. DRIMSeq: a Dirichlet-multinomial framework for multivariate count outcomes in genomics. F1000Res. 2016;5:1356.

82. Ogata H, Goto S, Sato K, Fujibuchi W, Bono H, Kanehisa M. KEGG: Kyoto Encyclopedia of Genes and Genomes. Nucleic Acids Res. 1999 Jan 1;27(1):29–34.

83. Mi H, Muruganujan A, Casagrande JT, Thomas PD. Large-scale gene function analysis with the PANTHER classification system. Nat Protoc. 2013 Aug;8(8):1551–66.

84. Nishimura D. BioCarta. Biotech Software & Internet Report. 2001 Jun 1;2(3):117–20.

85. Fabregat A, Jupe S, Matthews L, Sidiropoulos K, Gillespie M, Garapati P, et al. The Reactome Pathway Knowledgebase. Nucleic Acids Research. 2018 Jan 4;46(D1):D649–55.

86. Page MJ, McKenzie JE, Bossuyt PM, Boutron I, Hoffmann TC, Mulrow CD, et al. The PRISMA 2020 statement: an updated guideline for reporting systematic reviews. BMJ. 2021 Mar 29;372:n71.

87. Wickham H. ggplot2. WIREs Computational Statistics. 2011;3(2):180–5.

88. Simoes R de M, Emmert-Streib F. Bagging Statistical Network Inference from Large-Scale Gene Expression Data. PLOS ONE. 2012 Mar 30;7(3):e33624.

89. Tennekes M, de Jonge E. TOP-DOWN DATA ANALYSIS WITH TREEMAPS. 2011;6.

90. Liaw A, Wiener M. Classification and Regression by randomForest. R News. 2002;2(3):18–22.

91. Scott TM, Jensen S, Pickett BE. A signaling pathway-driven bioinformatics pipeline for predicting therapeutics against emerging infectious diseases. F1000Res. 2021;10:330.

92. naomi-rapier-sharman. summarize_Pathways2Targets2_output [Internet]. 2022 [cited 2022 Apr 15]. Available from: https://github.com/naomi-rapier-sharman/summarize_Pathways2Targets2_output

Supporting information captions

S0 File. B-Cell Non-Hodgkin's Lymphomas Transcriptomic Meta-Analysis: Supplementary Materials Description. This document contains a guide to allow readers to easily navigate the supplementary files.

S1 File. PRISMA 2020 checklist for transparent meta-analysis reporting. This document contains the PRISMA guidelines for reporting meta-analyses/systematic reviews and the manuscript location of required information.

S2 File. Differentially expressed gene results (edgeR output). The entire BCNHL differentially expressed gene list produced by edgeR. The file is written in TSV format and can be successfully opened in Excel. Some genes in the original TSV file have more associated data than can fit on one line. The genes in the file are ranked according to FDR, with the smallest FDRs at the top. Please note, the file also contains differential expression results for genes which were not significantly differentially expressed at the bottom. For description of column contents, please see S0 File.

S3 File. Differentially expressed splice variants (by gene; DRIMSeq output). The BCNHL differentially expressed splice variant results (by gene) produced by DRIMSeq. Genes are ranked according to adjusted p-value, with the lowest adjusted p-value at the top. NOTE: Should you desire to discover which transcripts of a certain gene are present in the BCNHL dataset, see the "tx_ids" column in Supplementary File S1. For description of column contents, please see S0 File.

S4 File. Differentially expressed gene ontology results (Camera output). The BCNHL differentially expressed gene ontology results produced by Camera. No gene ontologies were significant after performing the FDR correction. For description of column contents, please see S0 File.

S5 File. Differentially regulated pathway results (SPIA output). The BCNHL differentially expressed pathway results produced by SPIA. For description of column contents, please see S0 File.

S6 File. Drug prediction results by gene (Pathways2Targets unsorted output). The raw drug prediction results from Pathways2Targets2.R.

S7 File. Drug prediction results sorted by most significant pathways impacted (Pathways2Targets sorted output). The sorted drug prediction results, ranked according to which drugs impact the highest number of significantly modulated pathways.

S8 File. Biomarker prediction results (randomForest output). The ranked random forest biomarker prediction results. Sheet one contains all genes, and sheet two contains the random forest results when the selection was narrowed to the top three genes.

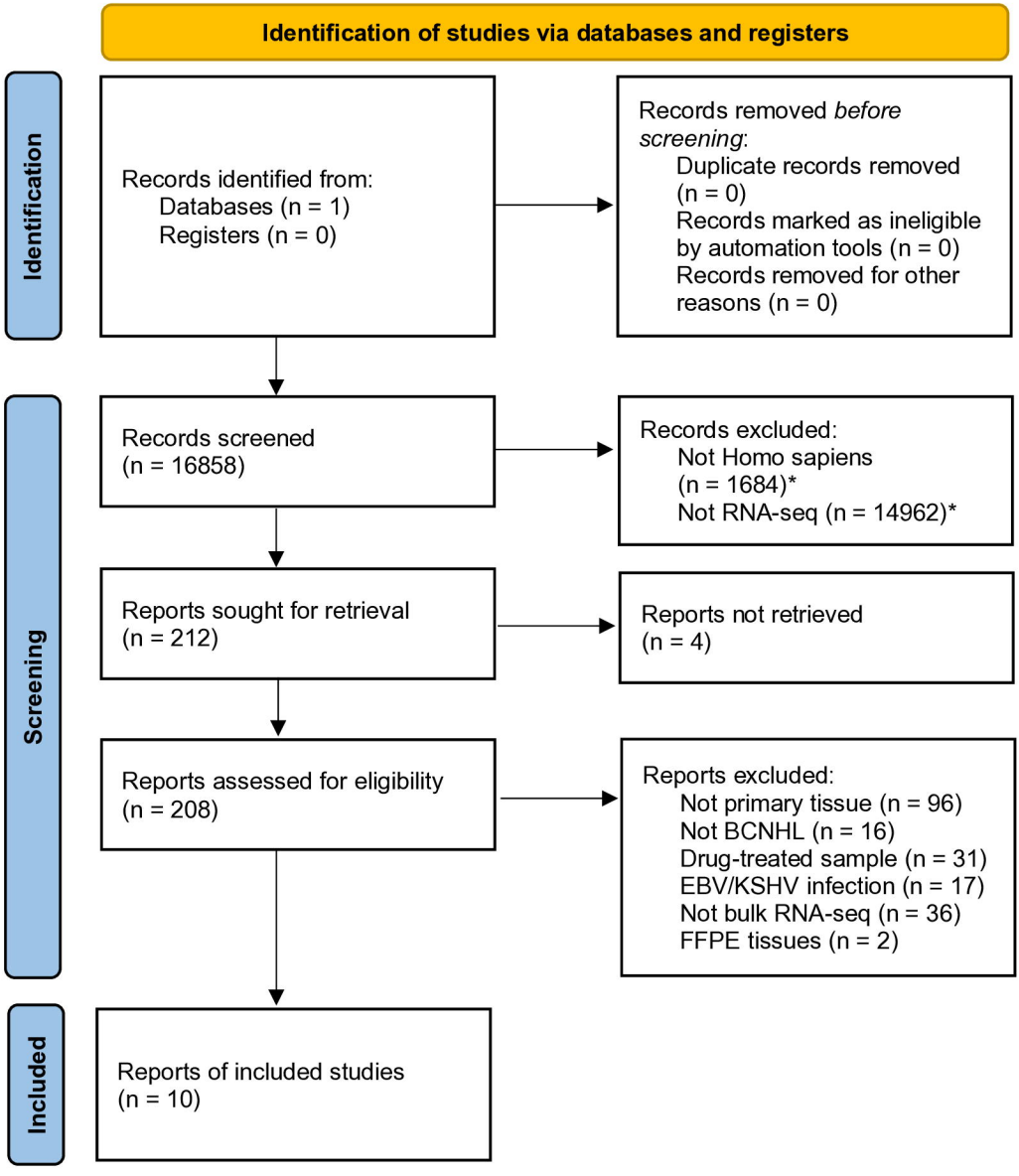

*Excluded by automation. All other excluded records were excluded by a human.

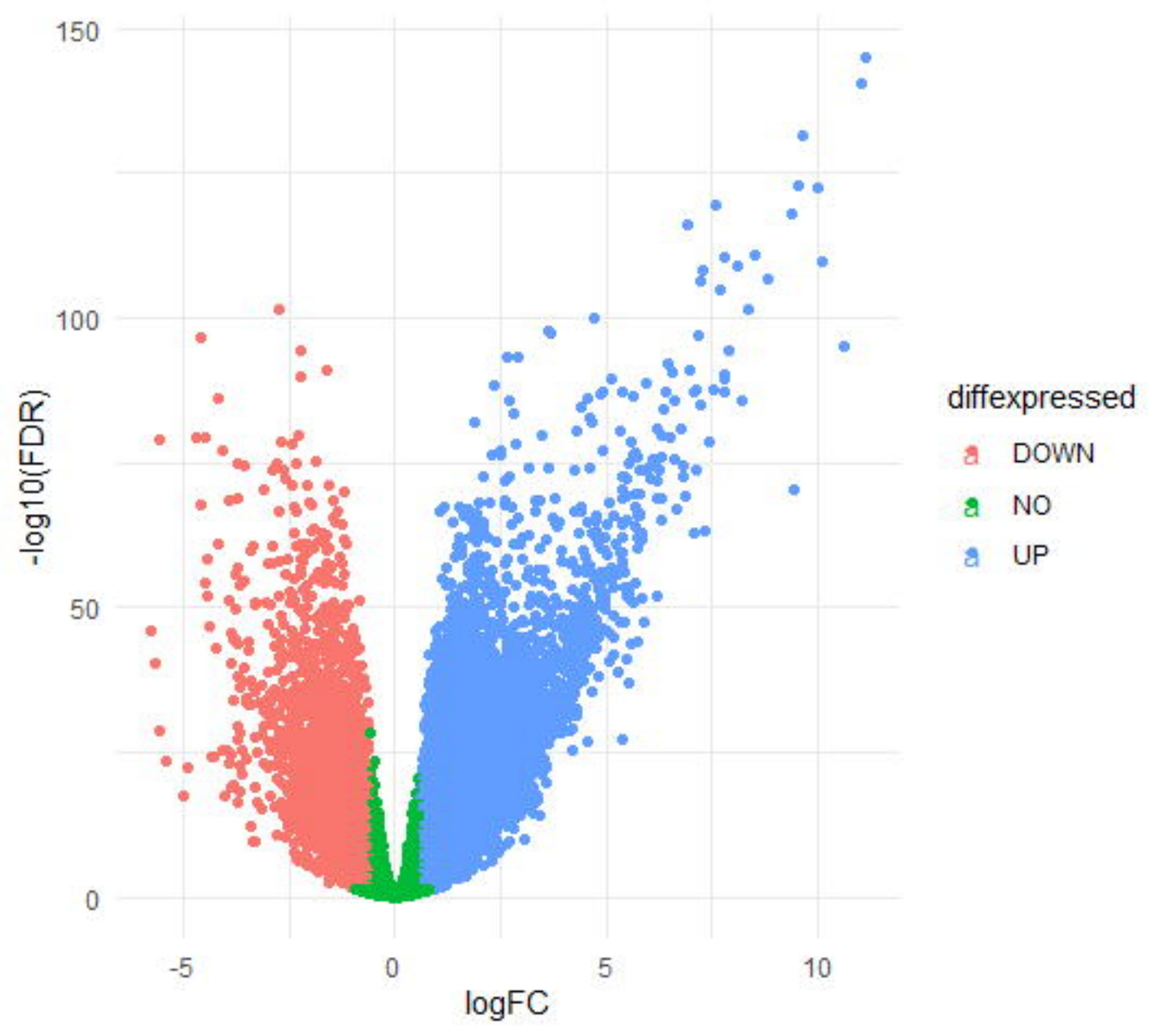
150
100
50
0
-log10(FDR)
-5
0
5
10
logFC
diffexpressed
DOWN
NO
UP

BCNHL vs. Healthy

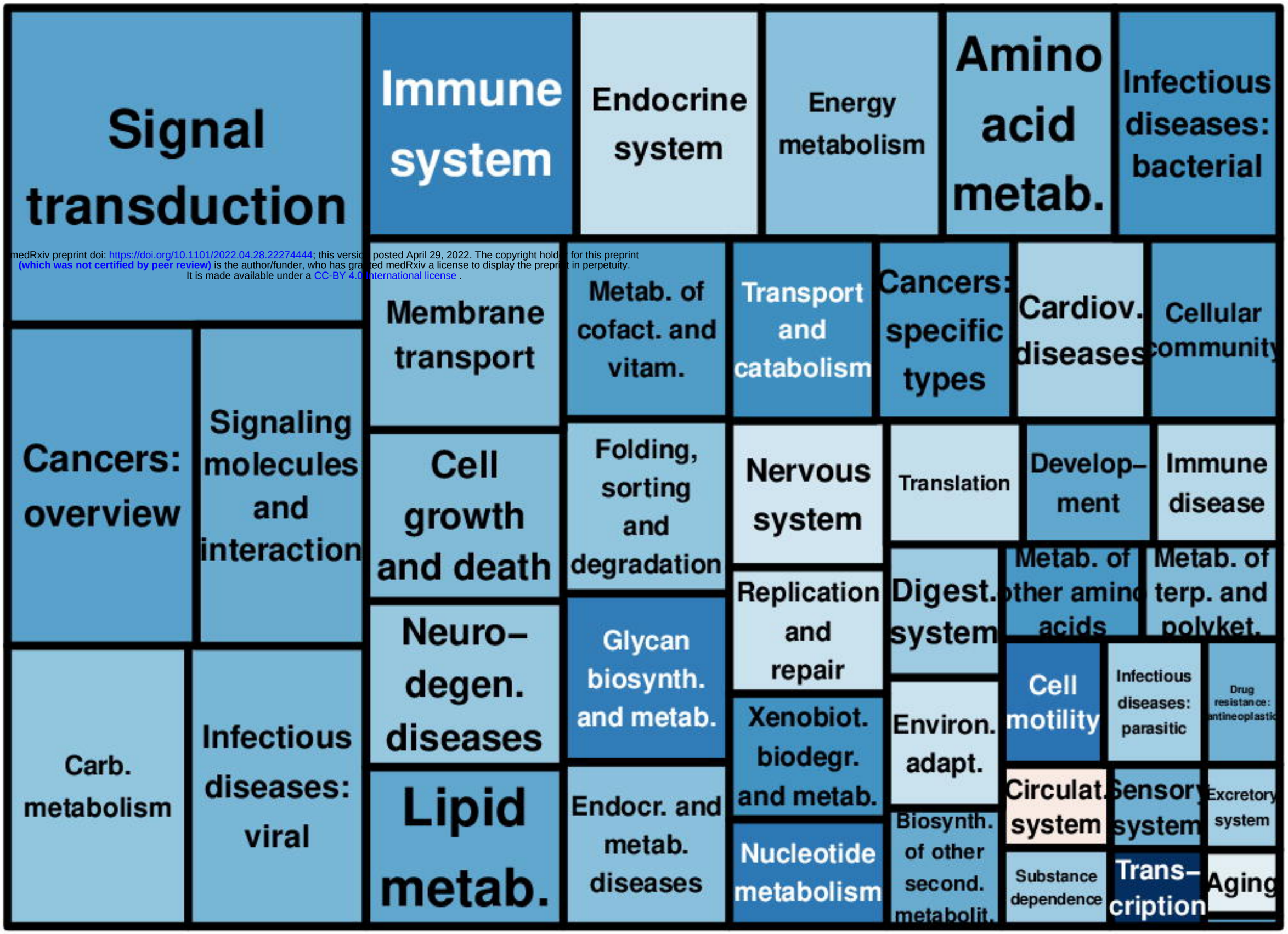

Average Log2 Fold Change

A

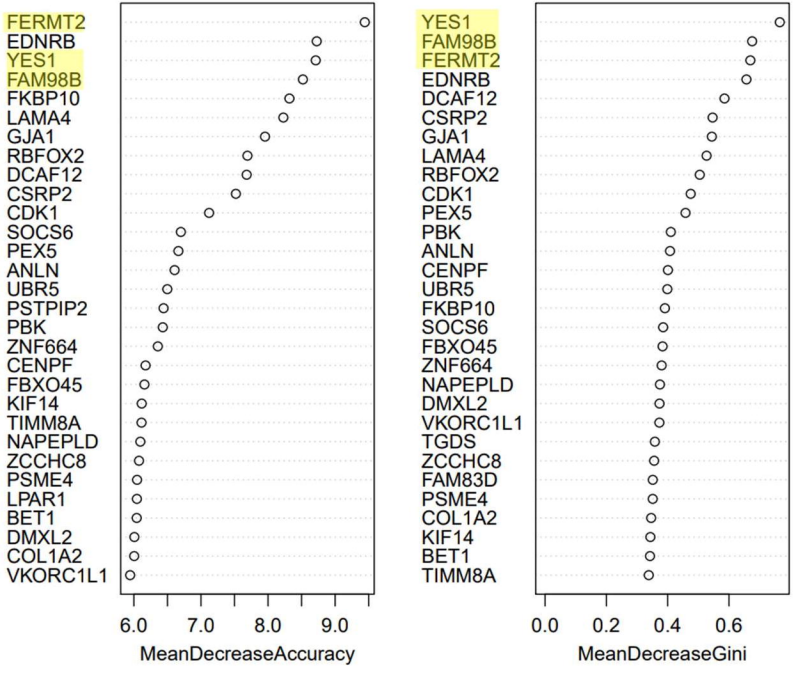
FERMT2
EDNRB
YES1
FAM98B
FKBP10
LAMA4
GJA1
RBFOX2
DCAF12
CSRP2
CDK1
SOCS6
PEX5
ANLN
UBR5
PSTPIP2
PBK
ZNF664
CENPF
FBXO45
KIF14
TIMM8A
NAPEPLD
ZCCHC8
PSME4
LPAR1
BET1
DMXL2
COL1A2
VKORC1L1
6.0
7.0
8.0
9.0
MeanDecreaseAccuracy
YES1
FAM98B
FERMT2
EDNRB
DCAF12
CSRP2
GJA1
LAMA4
RBFOX2
CDK1
PEX5
PBK
ANLN
CENPF
UBR5
FKBP10
SOCS6
FBXO45
ZNF664
NAPEPLD
DMXL2
VKORC1L1
TGDS
ZCCHC8
FAM83D
PSME4
COL1A2
KIF14
BET1
TIMM8A
0.0
0.2
0.4
0.6
MeanDecreaseGini

B

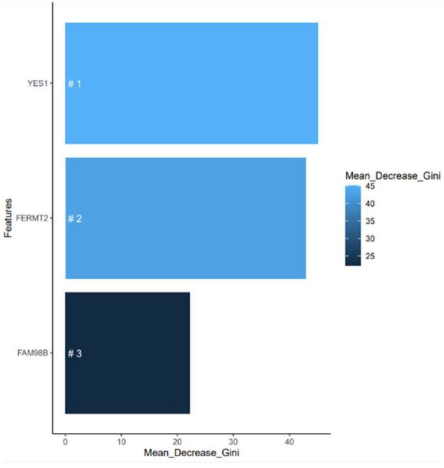
YES1
1
FERMT2
2
FAM98B
3
Features
Mean_Decrease_Gini
45
40
35
30
25
0
10
20
30
40
Mean_Decrease_Gini

ROC plot

C

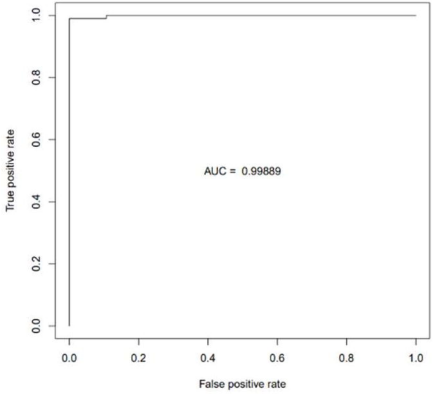
AUC = 0.99889
True posilive rate
False positive rate
0.0
0.2
0.4
0.6
0.8
1.0